Extended Hückel Theory for Quantum Transport in Magnetic Tunnel Junctions

Gautam Shine*, Sasikanth Manipatruni†, Anurag Chaudhry‡, Krishna C. Saraswat*,
Dmitri E. Nikonov†, Ian A. Young†

*Department of Electrical Engineering, Stanford University, Stanford, CA 94305 USA
†Components Research, Intel Corporation, Hillsboro, OR 97124 USA
‡Design Technology Solutions, Intel Corporation, Santa Clara, CA 95054 USA
gshine@stanford.edu

Abstract—**Spin-resolved conductivities in magnetic tunnel junctions are calculated using a semiempirical tight-binding model and non-equilibrium Green's functions. The performance of half-metallic electrodes is studied by comparing conventional Fe-MgO-Fe structures to Co_2FeAl-MgO-Co_2FeAl structures. The results show higher tunneling magnetoresistance and resistance-area product for Co_2FeAl devices across a wide bias range.**

I. INTRODUCTION

Spin-based memory and logic devices are a proposed replacement for charge-based devices as CMOS scaling becomes difficult. A critical component of many such spintronic devices is the magnetic tunnel junction (MTJ), a trilayer ferromagnet-insulator-ferromagnet stack. MTJs are capable of storing a logic state using the magnetization of electrodes. Parallel (P) and anti-parallel (AP) alignments present different resistances to current flow, known as tunneling magnetoresistance and defined as TMR = (R_{AP} - R_P) / R_P. This effect arises from the mismatch in the spin-dependent density of states and produces TMR of $\sim$50%. The discovery of symmetry filtering by lattice-matched MgO [1] due to coherent tunneling boosted experimental TMR to 600% in CoFeB-MgO-CoFeB [2].

This effect occurs because opposite spins have different orbital characters near the Fermi level. Specifically, majority spin electrons in Fe and Co are composed of Δ_1 symmetry Bloch waves, which match the MgO conduction and valence bands, while minority spin electrons are composed of Δ_2, $\Delta_{2'}$, and Δ_5 symmetries. Though all states are evanescent while tunneling, Δ_1 states decay at a much slower rate. Capturing this symmetry filtering in a model requires full-band quantum transport, implemented here in an atomistic simulator using semiempirical extended Hückel theory (EHT) for electronic structure and non-equilibrium Green's functions (NEGF) for transport. This method has been successfully used to simulate Fe-MgO-Fe MTJs [3][4]. Here we will apply it to the class of materials known as full Heusler alloys, particularly Co_2FeAl (CFA), which possesses a half-metallic band structure.

Despite the small number of parameters in EHT (3-5 per valence orbital), the method can produce excellent E-k fits and benefits from the natural exponential scaling of atomic interactions [5]. Since DFT commonly underestimates band gaps, EHT has the additional benefit of being able to fit to experimental gap values. This is especially important for tunneling calculations and is necessary for MgO, which has a band gap of $\sim$7.8 eV compared to $\sim$5.5 eV predicted by LDA.

The minority spin band gaps of full Heusler alloys are also subject to a similar error in DFT but the use of +U corrections produces more realistic values [6]. Current experimental results for MTJs with half-metallic electrodes are of comparable performance to those with conventional ferromagnetic electrodes like Fe and CoFe. This is not unexpected since their current state of fabrication is immature. We present here the theoretical performance of a CFA-MgO-CFA device to determine its usefulness, particularly at the read and write voltages to be used in future memory circuits.

II. METHODOLOGY

EHT uses an explicit basis set of Slater-type orbitals (STOs) to calculate overlap integrals and uses them to weight off-diagonal matrix elements. STOs are the product of radially decaying functions and spherical harmonics, resembling hydrogenoids but only possessing nodes for linear combinations. The fitting parameters are the onsite energies, the strengths of the radial decay, and the coefficients for linear combinations of STOs. Some simple orbitals such as the valence s and p orbitals of Mg and O can be represented by a single STO. The matrix elements are given by

$$H_{ii} = E_{onsite}$$
$$H_{ij} = K \, S_{ij} \, (H_{ii} + H_{jj})/2$$
$$S_{ij} = \langle \psi_i \, | \, \psi_j \rangle$$
$$\psi_{n,l,m} = c_1 R_{n,\zeta_1} Y_{l,m} + c_2 R_{n,\zeta_2} Y_{l,m}$$

K is a constant taken to be 2.3 in solids [5], $R_{n,\zeta}$ are radial functions simplified from Laguerre polynomials, and $Y_{l,m}$ are spherical harmonics. The Hamiltonian is assembled using an input atomic configuration with the potential U assumed to be flat in the metals and linear in the oxide, but with corrections for the non-orthogonality of the basis set.

We then use the Landauer approach with Green's functions to calculate the current [7]

$$J = \frac{q}{h} \int dE \, T(E) \, (f_1 - f_2)$$
$$T(E) = Tr[\Gamma_1 \, G \, \Gamma_2 \, G^\dagger]$$
$$G(E) = [(E + i0^+)S - H - U - \Sigma_1 - \Sigma_2]^{-1}$$

The self-energies $\Sigma = \tau g \tau^\dagger$ modify the Hamiltonian to account for the contacts and are calculated using surface Green's functions g obtained with the iterative Sancho-Rubio method [8]. The broadening matrices Γ are given by $i[\Sigma - \Sigma^\dagger]$.

The periodicity of the structure in the plane parallel to the interface allows the problem to be reformulated as a sum over independent conducting modes indexed by $k_\parallel = (k_x, k_y)$ where z is the direction of transport. The Hamiltonian can be Fourier transformed into momentum space as

$$H(\vec{k_\parallel}) = \sum_{\vec{r}} H(\vec{r})\, e^{i\vec{k_\parallel} \cdot \vec{r}}$$

The overlap and potential matrices are similarly transformed. The Green's functions, self-energies, and broadening matrices are then a function of $k_\parallel$. Summation of $T(E, k_\parallel)$ over the 2D transverse Brillouin zone approximates $T(E)$. A 101x101 k-point equivalent grid was used and the Fermi function is taken at T = 300 K.

III. RESULTS

We have benchmarked our simulator against results from DFT-NEGF and previous EHT-NEGF calculations. It was found that previous EHT-based calculations had poor orbital parameters for the MgO tunnel barrier and this resulted in higher current and lower TMR than expected when extrapolating from DFT-based calculations. Our improved parameters produce the correct slope for resistance-area (RA) v. t_{ox} plots, which is an important step for comparing with experiments. The TMR-V behavior is shown in Fig. 1 and the magnitude is significantly higher than previous results for 6+ MgO layers. This is due to better fits to the MgO E-k relation near the band minima, which determines the tunneling effective mass.
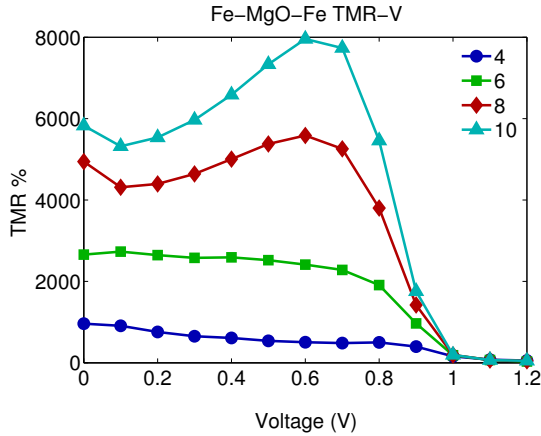

Fig. 1: TMR-V relation of Fe-MgO-Fe structures for 4 to 10 monolayers of MgO. These results are qualitatively similar to previous EHT-NEGF calculations but have higher TMR magnitudes for 6+ MgO layers.

In attempting to fit tight-binding parameters to CFA, we found that conventional EHT could not reproduce the CFA band structure, particularly the minority spin gap. This is due to EHT possessing only one onsite energy for each valence orbital. This degeneracy is accurate for spherically symmetric potentials and is a reasonable assumption for materials with no charge transfer (e.g. elemental solids), but not for CFA.

In CFA the minority spin gap is a consequence of the hybridization of Co's bonding t_{2g} orbitals (d_{xy}, d_{xz}, d_{yz}) and antibonding e_g orbitals (d_{z^2}, $d_{x^2-y^2}$) [9]. Parameterizing this crystal field splitting in a tight-binding representation requires having different onsite energies (diagonal elements) for the corresponding spherical harmonics. Fig. 2 shows our E-k fits for CFA majority and minority bands following this modification for the 3d orbitals of Co and Fe.
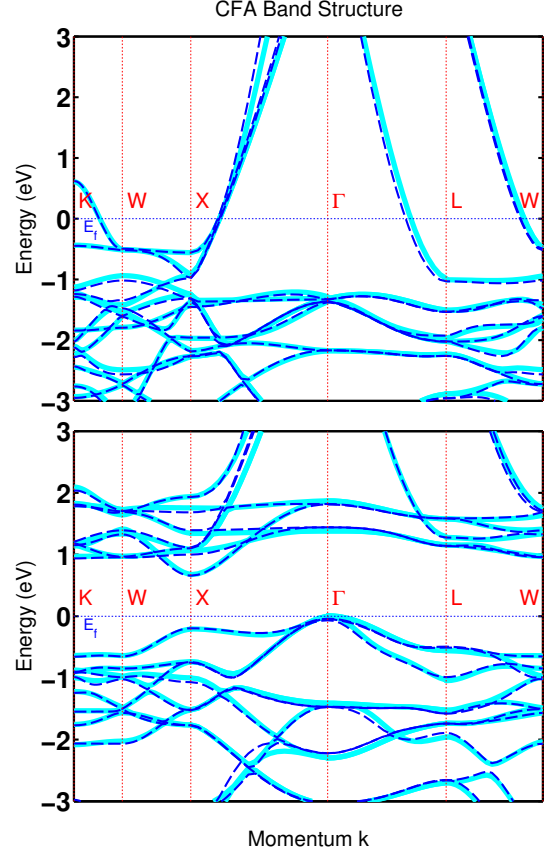

Fig. 2: Band structure of Co_2FeAl majority (top) and minority (bottom) electrons in EHT (dashed) and LDA+U (solid). Obtaining this accurate fit in EHT requires symmetry-resolved onsite energies for the Co and Fe 3d orbitals to account for crystal field splitting.

With optimized parameters for both MgO and CFA, we calculated transport in the full CFA-MgO-CFA structure. As expected, TMR diverges at low biases because of the half-metallicity of the CFA bands. This is not seen experimentally and a variety of reasons have been proposed including defects, non-collinear interface spins [10], spin wave excitations [11], and processes that introduce gap states and destroy half-metallicity at room temperature [12]. However, recent experimental results have shown that similar compounds $Co_2FeAl_{0.5}Si_{0.5}$ [11] and Co_2MnSi [13] retain their half-metallicity at room temperature.

Our primary interest is in device behavior at bias levels corresponding to read and write signals in future memory circuits (0.1 - 0.6 V). Fig. 3 shows the TMR-V and J-V behavior of Fe-MgO-Fe and CFA-MgO-CFA structures with 4 MgO layers. The parallel current is lower in CFA devices by a factor of 2 to 4 while the anti-parallel current is lower by over an order of magnitude until the bias passes ∼0.7 V.

The net effect relative to conventional Fe-MgO-Fe devices is superior TMR at relevant biases but at the expense of a higher RA product and much more variation of TMR with bias. Real devices are leakier than the perfect crystals modeled here, particularly in the AP configuration where CFA's advantage lies. Partial demagnetization at finite temperatures also contributes to lowering TMR and affects CFA more than Fe due to its intrinsically higher spin polarization.
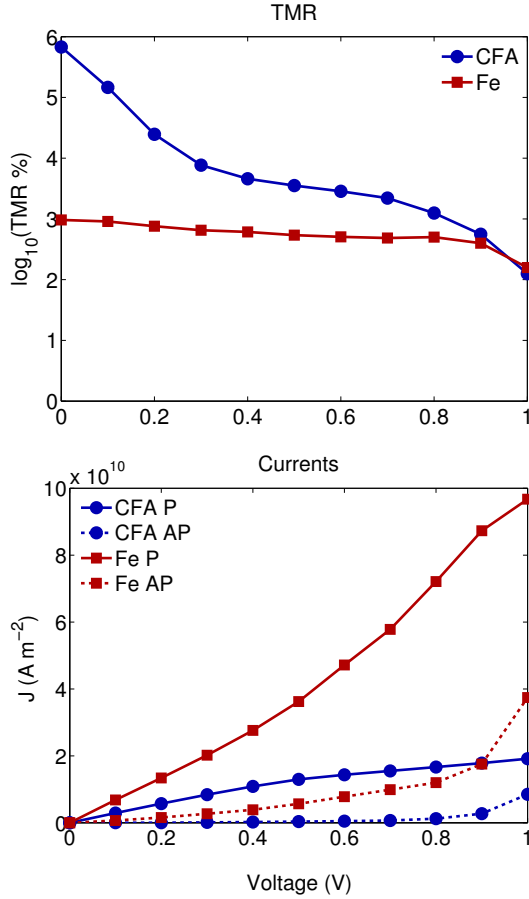

Fig. 3: TMR-V (top) and J-V (bottom) for MTJs with Fe and CFA electrodes. The half-metallicity of CFA allows it to suppress AP current more effectively than Fe until high biases. This results in much higher TMR but the RA product of the CFA device is also higher and the variation of TMR with bias is more drastic.

The 2D Brillouin zone's $k_\parallel$-dependence of transmission at the Fermi level is shown in Fig. 4. For majority electrons in the parallel configuration, CFA devices show the same broad Γ-centered transmission peak of Δ_1 states seen in Fe and CoFe devices. The difference arises in the parallel minority and anti-parallel transmission, both of which are several orders of magnitude lower due to the absence of minority spin states near the Fermi level.

IV. CONCLUSION

We have simulated quantum transport in Fe-MgO-Fe and CFA-MgO-CFA heterostructures using EHT and NEGF. By allowing symmetry-resolved onsite energies, EHT is capable of accurately modeling the band structure of full Heusler alloys including the critical minority spin gap. The results show that a CFA device outperforms a Fe device in TMR across a wide
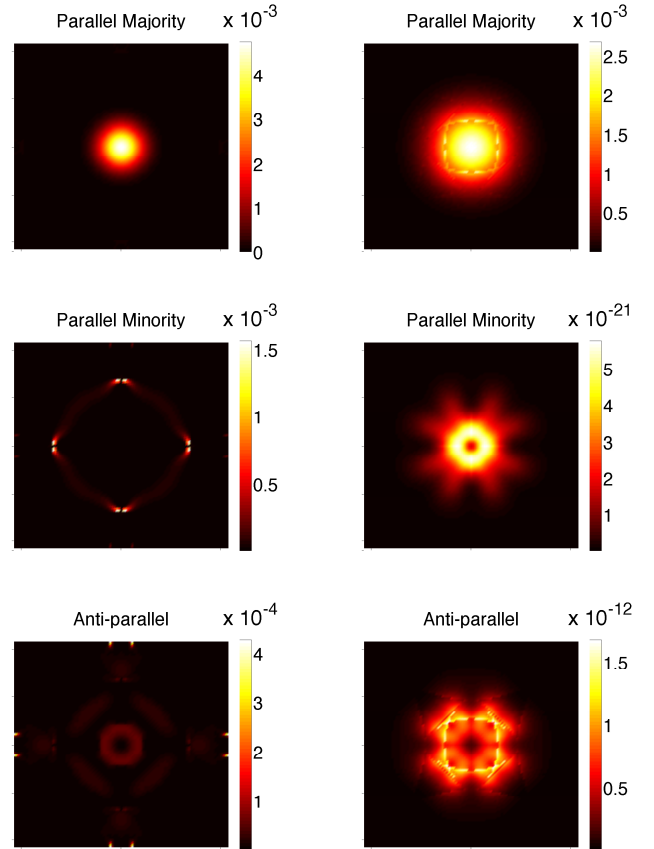

Fig. 4: Transmission at the Fermi level in the transverse Brillouin zone of Fe-MgO-Fe (left) and CFA-MgO-CFA (right) with 4 MgO layers. For parallel majority (top), both structures show a broad transmission peak centered around the Γ-point characteristic of Δ_1 states. Parallel minority (middle) and anti-parallel (bottom) show much lower transmission magnitudes, particularly for the CFA device.

bias range due to better AP current suppression. However, its resistance-area product is also higher and TMR shows greater variation with bias.

REFERENCES

[1] W. H. Butler et al., Phys. Rev. B 63, 054416 (2001).
[2] S. Ikeda et al., Appl. Phys. Lett. 93, 082508 (2008).
[3] T. Z. Raza et al., J. Appl. Phys. 109, 023705 (2011).
[4] A. M. Roy et al., J. Appl. Phys. 112, 104510 (2012).
[5] J. Cerdá et al., Phys. Rev. B 61, 79657971 (2000).
[6] G. H Fecher et al., J. Phys. D: Appl. Phys. 40, 1582 (2007).
[7] S. Datta, Quantum Transport: Atom to Transistor, (2005).
[8] M. P. López-Sancho et al., J. Phys. F 15, 851 (1985).
[9] I. Galanakis et al., Phys. Rev. B 66, 174429 (2002).
[10] Miura et al., Phys. Rev. B 83, 214411 (2011).
[11] R. Shan et al., Phys. Rev. Lett. 102, 246601 (2009).
[12] L. Chioncel et al., Phys. Rev. Lett. 100, 086402 (2008).
[13] M. Jourdan et al., Nat. Commun. 5, 3974 (2014).